Magnetic properties of transition-metal impurities in silicon quantum dots

Li Ma,[1,2] Jijun Zhao,[1,*] Jianguang Wang,[2] Baolin Wang,[2] and Guanghou Wang[2]
[1]*State Key Laboratory of Materials Modification by Laser, Electron, and Ion Beams, School of Physics and Optoelectronic Technology and College of Advanced Science and Technology, Dalian University of Technology, Dalian 116024, China*
[2]*National Laboratory of Solid State Microstructures and Department of Physics, Nanjing University, Nanjing 210093, China*
(Received 26 January 2006; published 8 January 2007)

First-principles calculations have been conducted to investigate the magnetic properties of 3*d* and 4*d* transitional-metal (TM) atoms doped in hydrogen-passivated silicon quantum dots. The TM impurities exhibit almost identical magnetic behavior in the quantum dots of different sizes. The magnetic moments for most 3*d* and 4*d* TM atoms are completely quenched by the silicon hosts, while the magnitudes of the remaining moments for V, Cr, Mn, Nb, Mo, and Tc impurities are significantly reduced from those of free atoms. The moments of these 3*d* atoms are higher than those of the 4*d* atoms of the same family. Doping of TM atoms in different sites of lattice and the dopants of more than one atom are also considered. The structural and bonding properties of the TM-doped silicon quantum dots are discussed. The finding of magnetic properties makes them attractive for developing nanoscale magnetic species for spintronics.

DOI: 10.1103/PhysRevB.75.045312 PACS number(s): 73.21.La, 73.20.Hb, 75.75.+a

I. INTRODUCTION

Doping—the intentional introduction of impurities into a material—is a fundamental approach for controlling the properties of bulk semiconductors. It is well known that reducing the dimension of a semiconductor solid into nanometer scale would lead to fundamental changes in its physical properties.[1] This has stimulated similar efforts to dope semiconductor nanocrystals.[2] However, little is known about the magnetic properties of silicon quantum dots doped with transitional metal (TM) atoms from a theoretical point of view. Since silicon is the backbone of modern microelectronic industry, it is desirable to develop silicon-based spintronics that can be directly integrated with existing silicon technologies.[3]

Over the last decade, hydrogen passivated Si_nH_m clusters as a prototype of semiconductor quantum dots have become the subjects of intensive experimental[4,5] and theoretical[6–11] studies. Most of these works focused on electronic and optical properties[1,10,11] of pristine Si_nH_m quantum dots. However, what is the magnetic behavior of a transition-metal atom when it is doped in Si_nH_m quantum dots? The answer to this question and the relevant investigations on the dilute magnetic semiconductor nanostructures are of obvious importance to the emerging fields of spintronics and nanoelectronics.

It is well known that the 3*d* transition metal atoms Sc, Ti, V, Cr, Mn, Fe, Co, and Ni possess magnetic moments of $1\mu_B$, $2\mu_B$, $3\mu_B$, $6\mu_B$, $5\mu_B$, $4\mu_B$, $3\mu_B$, and $2\mu_B$, respectively. When they are deposited on the metal substrates, such as Ag(001), Cu(001), Pd(001), and Pt(001), the local magnetic moment of the adsorbed atom raises from Sc to Cr and declines from Mn to Ni, irrespective of the metal host.[12] Although the variation in the magnetic moments of the absorbed TM atoms follows the same trend in the free atoms, the magnitudes of their magnetic moments are significantly lower than their free-atom values.[12] For the 4*d* TM metal clusters on a Ag(001) surface, the moments of the early transition elements are quenched and the maximum of moment is shifted to higher valences.[12] For bulk ZnO solid doped by 3*d* or 4*d* transition metals ($TM_{0.25}Zn_{0.75}O$), the computed magnetic moments of Ti, Cr, Mn, Fe, Co, Ni, Ru, Pd, and Ag impurities in the systems were $1.24\mu_B$, $3.78\mu_B$, $4.93\mu_B$, $4.24\mu_B$, $3.00\mu_B$, $2.00\mu_B$, $0.74\mu_B$, $1.00\mu_B$, and $0.00\mu_B$, respectively.[13] When supported on an organic molecule such as benzene,[14] the magnetic moments for Sc, Ti, and V atoms are enhanced by $2\mu_B$, while those of Mn, Fe, Co, and Ni atoms are reduced by $2\mu_B$ from their free-atom values; especially, the magnetic moment of Ni is completely quenched. The magnetic moment of Cr atom remains unchanged when it is supported on benzene, namely at $6\mu_B$, whereas the magnetic moment of Cr atom is completely quenched when it is encapsulated in silicon cages.[15] Our recent first-principles calculations on the Fe-doped silicon $FeSi_n$ clusters showed that the magnetic moment on the Fe atom is completely quenched as the cluster size exceed $n=9-10$.[16] All of these results indicate that the magnetic behavior of a TM atom sensitively depends on the interaction between the TM atom and the host. In this work, we report a computational study of the magnetic properties of Si_nH_m quantum dots doped by a series of 3*d* and 4*d* TM atoms.

II. THEORETICAL METHODS

The initial configurations of spherical-like Si_nH_m clusters were constructed by symmetrically cutting the bulk diamond structure of silicon. Si_nH_m clusters of different sizes and shapes, such as Si_5H_{12}, $Si_{17}H_{36}$, $Si_{29}H_{36}$, $Si_{35}H_{36}$, $Si_{59}H_{60}$, $Si_{75}H_{76}$, and $Si_{123}H_{100}$, have been considered. The dangling bonds of the surface Si atoms of the nanocrystallines were fully passivated by hydrogen atoms. For most of the systems studied, a transition-metal atom was substitutionally doped in the central Si site of the Si_nH_m clusters, whereas the $Si_{n-1}H_m$ clusters with a central vacancy were also investigated for comparison. For some selected cases, we considered different doping sites other than the cluster center and investigated the magnetic behavior of quantum dots with more than one TM dopant.

After the initial configurations were constructed, geometry optimizations were performed using spin-polarized density functional theory (DFT) implemented in a DMOL

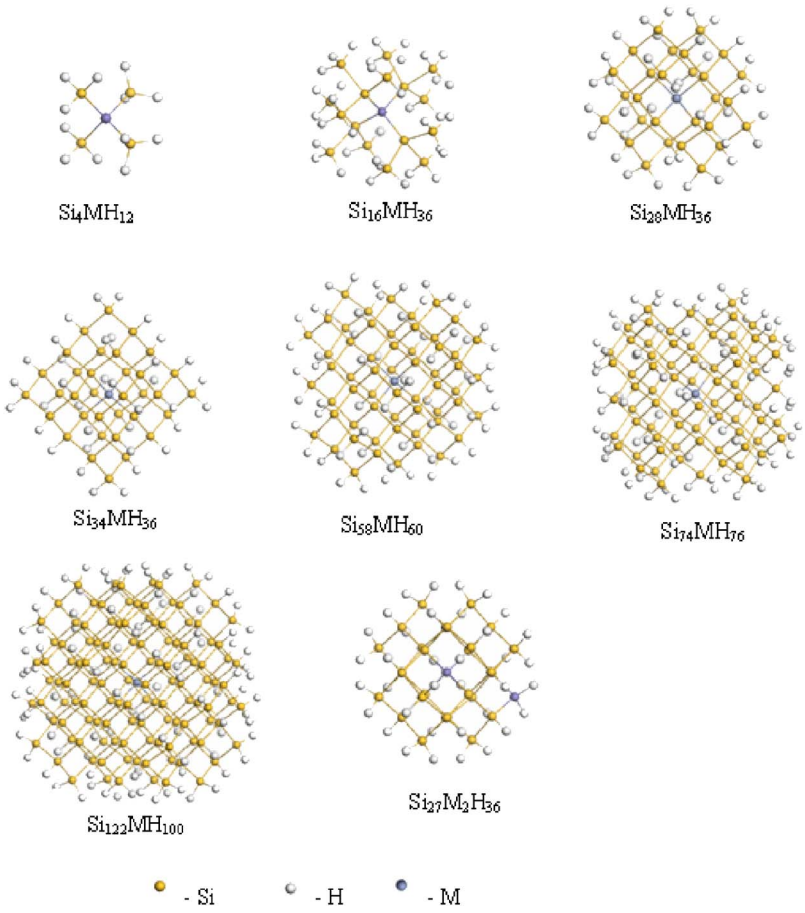

FIG. 1. (Color online) Equilibrium structures of $Si_{n-1}MH_m$ and $Si_{27}M_2H_{36}$ clusters.

package.[17] In the DFT calculations, all-electron treatment and double numeric basis set including *p*-polarization function (DNP) (Ref. 17) were chosen. The exchange-correlation interaction was treated by the generalized gradient approximation (GGA) with the functional parameterized by Perdew, Burke, and Enzerhof (PBE).[18] Spin-polarized self-consistent field calculations were done with a convergence criterion of 10^{-6} hartree on the total energy. All the structures were fully optimized without any symmetry constraint with a convergence criterion of 0.002 hartree/Å for the forces and 0.005 Å for the displacement. The equilibrium structures of $Si_{n-1}MH_m$ ($M=3d$, $4d$ transition metals) clusters are shown in Fig. 1.

III. RESULTS AND DISCUSSION

A. Magnetic properties of individual TM impurity in the center site

As the simplest case, we first consider the substitutional doping of an individual in the center site of a silicon quantum. To investigate the trend of the transition-metal elements across the periodic table, we computed the magnetic properties of the $3d$ and $4d$ TM impurities inside two representative quantum dots, i.e., $Si_{29}H_{36}$ and $Si_{59}H_{60}$. The local magnetic moments on the TM atoms in the center of silicon quantum dots from our calculations are summarized in Table I and Fig. 2. Most interestingly, we found that the magnetic moments of the impurity atoms of $3d$ (Sc, Ti, Fe, Co, Ni) and $4d$ (Y, Zr, Ru, Rh, Pd) transition metals are completely quenched in the silicon quantum dots. Meanwhile, other $3d$ and $4d$ transition-metal atoms such as V, Cr, Mn, Nb, Mo, and Tc doped inside silicon quantum dots remain magnetic, whereas the magnitudes of the magnetic moment are substantially reduced with regard to their atomic values. To confirm the present theoretical finding and to further investigate the magnetic behavior of these $3d$ and $4d$ impurities (V, Cr, Mn, Nb, Mo, Tc) inside silicon quantum dots, we also considered the clusters of different sizes (Si_5H_{12}, $Si_{17}H_{36}$, $Si_{35}H_{36}$, $Si_{75}H_{76}$, and $Si_{123}H_{100}$) doped with these TM atoms, and the details of those results will be discussed later.

Figure 2 shows the computed local moments for all of $3d$ and $4d$ TM atoms in $Si_{28}MH_{36}$ and $Si_{58}MH_{60}$ ($M=3d$, $4d$ transition metals) quantum dots. Across the periodic table, atoms of $3d$ and $4d$ TM elements belonging to the same family in the periodic table exhibit similar trends of magnetic behaviors, regardless the size of the silicon quantum dot hosts. For all the cases, the magnetic moments of the TM atoms are either totally quenched or significantly reduced due to the silicon host. Among the $3d$ ($4d$) elements, Cr (Mo) has the largest free-atom magnetic moment, i.e., $6\mu_B$. After being doped in Si_nH_m clusters, they still possess the largest magnetic moments among the $3d$ ($4d$) elements, about $2.8\mu_B$ and $2.0\mu_B$, respectively. For the $3d$ atoms, the moment of V ($3\mu_B$) is less than that of Mn ($5\mu_B$) by $2\mu_B$ in free atom. The same trend remains in TM-doped silicon quantum dots, but the difference of their magnetic moments reduces to only $0.3\mu_B$. Dramatic changes of magnetic behavior were observed for the doped Fe and Co atoms. In the

TABLE I. Heat of formation, local magnetic moment on TM atom, atomic charges on central TM site, and bond length between centered atom and the nearest Si atoms of 3*d* and 4*d* atoms in $Si_{n-1}MH_m$ clusters.

Cluster	Heat of formation (eV)	Magnetic moment (μ_B)	Charge	Bond length (Å)
$Si_{28}ScH_{36}$	−6.318	0	0.569	2.706
$Si_{28}TiH_{36}$	−7.394	0	0.454	2.553
$Si_{28}VH_{36}$	−6.433	1.346	0.296	2.474
$Si_{28}CrH_{36}$	−5.449	2.820	0.151	2.439
$Si_{28}MnH_{36}$	−5.417	1.715	0.042	2.354
$Si_{28}FeH_{36}$	−6.954	0	0.033	2.298
$Si_{28}CoH_{36}$	−7.271	−0.001	−0.149	2.281
$Si_{28}NiH_{36}$	−6.540	0.028	−0.035	2.305
$Si_{28}CuH_{36}$	−4.651	0	−0.081	2.387
$Si_{28}ZnH_{36}$	−3.035	0	0.069	2.483
$Si_{28}YH_{36}$	−6.384	0	0.692	2.839
$Si_{28}ZrH_{36}$	−7.987	0	0.583	2.676
$Si_{28}NbH_{36}$	−7.463	1.074	0.353	2.565
$Si_{28}MoH_{36}$	−6.924	2.105	0.176	2.494
$Si_{28}TcH_{36}$	−8.142	0.900	0.005	2.408
$Si_{28}RuH_{36}$	−9.253	0	−0.108	2.358
$Si_{28}RhH_{36}$	−7.971	0	−0.142	2.371
$Si_{28}PdH_{36}$	−5.126	0	−0.058	2.441
$Si_{28}AgH_{36}$	−3.225	0	0.096	2.580
$Si_{28}CdH_{36}$	−2.529	0	0.180	2.675
$Si_{58}ScH_{60}$	−6.327	0	0.793	2.659
$Si_{58}TiH_{60}$	−7.388	0	0.608	2.538
$Si_{58}VH_{60}$	−6.474	1.365	0.415	2.469
$Si_{58}CrH_{60}$	−5.489	2.886	0.260	2.441
$Si_{58}MnH_{60}$	−5.339	1.671	0.125	2.365
$Si_{58}FeH_{60}$	−6.964	0	0.107	2.318
$Si_{58}CoH_{60}$	−7.319	0.001	−0.072	2.303
$Si_{58}NiH_{60}$	−6.668	0	0.039	2.325
$Si_{58}CuH_{60}$	−4.842	0	0.005	2.395
$Si_{58}XnH_{60}$	−3.191	0	0.165	2.471
$Si_{58}YH_{60}$	−6.241	0	1.099	2.775
$Si_{58}ZrH_{60}$	−7.911	0	0.838	2.641
$Si_{58}NbH_{60}$	−7.391	1.080	0.554	2.548
$Si_{58}MoH_{60}$	−6.983	2.083	0.331	2.487
$Si_{58}TcH_{60}$	−8.103	0.978	0.126	2.412
$Si_{58}RuH_{60}$	−9.305	0	−0.011	2.368
$Si_{58}RhH_{60}$	−8.090	0	−0.040	2.379
$Si_{58}PdH_{60}$	−5.317	0	0.056	2.441
$Si_{58}AgH_{60}$	−3.391	0	0.251	2.553
$Si_{58}CdH_{60}$	−2.574	0	0.352	2.625
Si_4VH_{12}	−6.276	1.367	0.286	2.478
Si_4CrH_{12}	−5.283	2.858	0.134	2.443
Si_4MnH_{12}	−5.257	1.571	0.102	2.365
Si_4NbH_{12}	−7.215	1.138	0.336	2.572
Si_4MoH_{12}	−6.714	2.260	0.164	2.513
Si_4TcH_{12}	−7.858	1.087	0.013	2.428
$Si_{16}VH_{36}$	−6.278	1.467	0.266	2.475
$Si_{16}CrH_{36}$	−5.312	2.983	0.143	2.437
$Si_{16}MnH_{36}$	−5.296	1.704	0.039	2.351
$Si_{16}NbH_{36}$	−7.358	1.158	0.335	2.578
$Si_{16}MoH_{36}$	−6.821	2.231	0.168	2.502
$Si_{16}TcH_{36}$	−7.899	0.929	0.021	2.439
$Si_{34}VH_{36}$	−6.280	1.341	0.320	2.471
$Si_{34}CrH_{36}$	−5.293	2.805	0.172	2.435
$Si_{34}MnH_{36}$	−5.269	1.690	0.065	2.349
$Si_{34}NbH_{36}$	−7.322	1.068	0.374	2.565
$Si_{34}MoH_{36}$	−6.772	2.102	0.197	2.493
$Si_{34}TcH_{36}$	−7.990	0.893	0.029	2.406
$Si_{74}VH_{76}$	−6.425	1.360	0.399	2.464
$Si_{74}CrH_{76}$	−5.448	2.858	0.240	2.432
$Si_{74}MnH_{76}$	−5.343	1.654	0.101	2.354
$Si_{74}NbH_{76}$	−7.384	1.039	0.540	2.531
$Si_{74}MoH_{76}$	−6.986	1.988	0.175	2.461
$Si_{74}TcH_{76}$	−8.222	0.807	0.105	2.400
$Si_{122}VH_{100}$	−6.435	1.347	0.368	2.456
$Si_{122}CrH_{100}$	−5.281	2.614	0.058	2.408
$Si_{122}MnH_{100}$	−5.259	1.615	−0.110	2.334
$Si_{122}NbH_{100}$	−7.314	0.974	0.295	2.509
$Si_{122}MoH_{100}$	−7.045	2.033	0.269	2.464
$Si_{122}TcH_{100}$	−8.102	0.738	−0.025	2.387

cases of free atoms, the moments of Fe and Co are as high as $4\mu_B$ and $3\mu_B$, comparable to $3\mu_B$ of V atom, while both of them are totally quenched in Si_nH_m. The magnetic moments of the rest of the 3*d* free atoms (Sc, Ti, and Ni) are less than those of above-mentioned atoms and all of them are also quenched in Si_nH_m. Those 4*d* elements exhibit slightly different behavior from that of 3*d* elements in the same family. Free Nb and Tc atoms have the same magnetic moments ($5\mu_B$). After being doped in Si_nH_m, the moment of Nb is slightly larger than that of Tc by $0.1\mu_B$ to $0.2\mu_B$. The moments of other free atoms of 4*d* elements are less than the above-mentioned three atoms of Mo, Nb, and Tc, whereas the magnetic moments of them are all totally quenched in Si_nH_m.

Careful examinations show that the residual magnetic moments for 3d elements in silicon quantum dots are higher than those of the 4d elements belonging to the same family. This effect can be attributed to the fact that the 3d wave function is more localized.[12] For the other sized quantum dots studied (Si_4MH_{12}, $Si_{16}MH_{36}$, $Si_{34}MH_{36}$, $Si_{74}MH_{76}$, and $Si_{122}MH_{100}$), the TM atoms (V, Cr, Mn, Nb, Mo, Tc) with

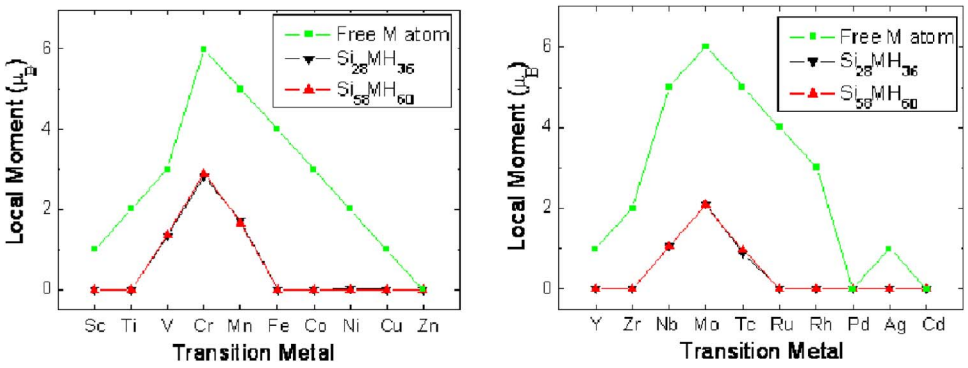

FIG. 2. (Color online) Local moments for $3d$ and $4d$ transitional metal atoms in $Si_{n-1}MH_m$ clusters. The magnetic moments of free atoms are also plotted for comparison.

residual magnetic moments exhibit magnetic behaviors that are similar to the results discussed above. As shown in Table I, Cr (Mo) still has the largest moment. The moment of V ($\sim 1.3\mu_B$) is slightly less than that of Mn ($\sim 1.6\mu_B$) and the moment of Nb ($\sim 1.0\mu_B$) is slightly larger than that of Tc ($\sim 0.8\mu_B$). Thus, our calculations suggest that the size and shape of the structural models used for the quantum dots have little effect on the magnetic properties of the TM impurity.

B. TM impurities at different sites in silicon quantum dots

In addition to doping at the center site of clusters, we considered the possibility for the TM dopants located at other substitutional sites. Due to the tremendous computational cost, we only studied Fe and Mn atoms as representatives of all $3d$ and $4d$ transition metal elements. They are substitutionally doped in different lattice sites of $Si_{28}FeH_{36}$, $Si_{28}MnH_{36}$, and $Si_{58}MnH_{60}$ respectively, from the center to the outermost site. Figure 3 presents the relative energy $E - E_{center}$ (given by the total energy of the dot with TM dopant at any site substrate the total energy of the quantum dot with TM dopant in the center) as function of the substitutional site. It can be clearly seen that TM atom prefers to stay in the central site. At all the doping sites, the magnetic moment of Fe atom is zero. For Mn dopant, the computed local moment is larger in the center than in other sites.

Besides the substitutional sites, it is also possible to dope the TM atoms in the interstitial positions. In Ref. 3, it was shown that Mn ions prefer tetrahedral interstitial positions in bulk Si solid. Here, we also consider the tetrahedral interstitial positions ($Si_{29}MH_{36}$) for Mn and Fe doping. The heat of formation of a TM-doped cluster can be calculated from the

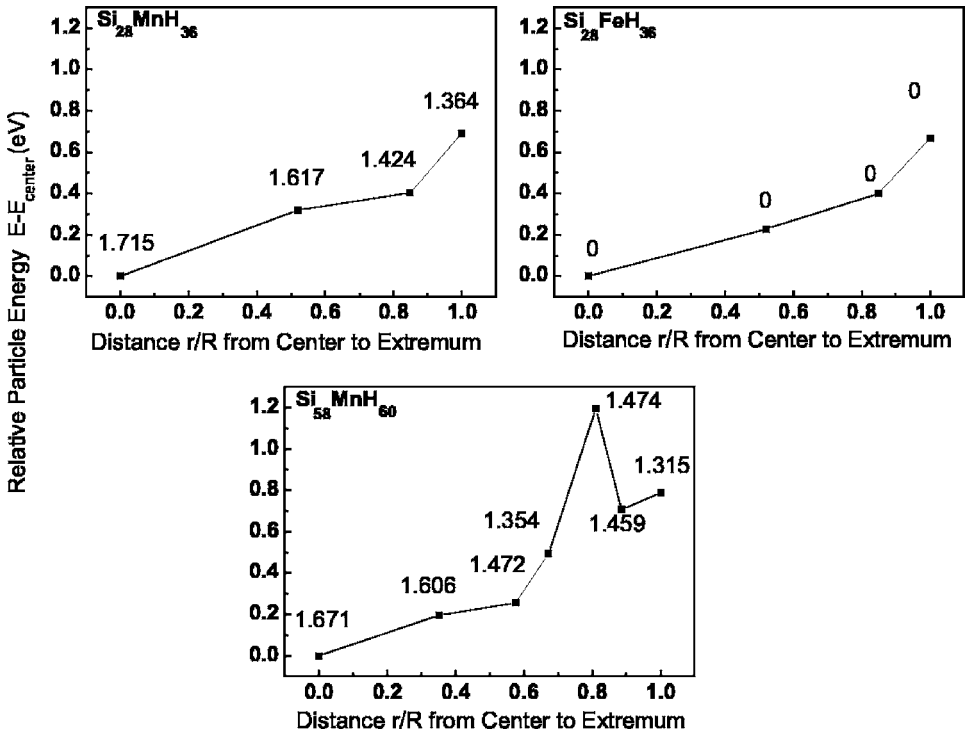

FIG. 3. Relative energy $E - E_{center}$ for each substitutional site of $Si_{28}MnH_{36}$, $Si_{28}FeH_{36}$, and $Si_{58}MnH_{60}$. The dimensionless radius r/R is obtained by dividing the distance from the center to the dopant site by the total distance from the center to the extremum. Hence $r/R=0$ is the center, and $r/R=1$ is the outermost dopant site located on an extremum. The number at each site is the local moment for metal atom, and the unit for it is μ_B.

TABLE II. Total energy relative to that of the lowest energy structure, spin of TM atom, and HOMO-LUMO gap for two Mn and two Fe atoms doping in $Si_{27}M_2H_{36}$.

$Si_{27}M_2H_{36}$	E_{tot} (eV)	Spin (μ_B)	Gap (eV)
Mn-Mn (a)	0.800	3.085 −1.581	0.342
Mn-Mn (b)	0.422	3.902 0.195	0.712
Mn-Mn (c)	0	3.295 0.873	0.624
Fe-Fe (a)	0	2.199 2.116	0.629
Fe-Fe (b)	0.587	0	1.284
Fe-Fe (c)	0.917	0	1.588

difference between the total energy of the doped cluster and the sum of the total energies of the corresponding pristine cluster and an isolated TM atom (negative value of heat of formation means exothermal and positive one denotes endothermal). The heats of formation for interstitial doping of Mn or Fe atom in the $Si_{29}H_{36}$ cluster are −1.320 eV and −2.703 eV, respectively, compared to the heat of formation for a Mn or Fe impurity (−5.417 eV and −6.954 eV, respectively) in the $Si_{28}H_{36}$ cluster with a central vacancy (Table I). In other words, the tetrahedral interstitial doping is less energetically preferred than the doping in vacancy site. From the above calculations, we argue that the center substitutional site is the most energetically preferred for TM doping.

We have also considered the silicon quantum dots with more than one dopant by calculating the magnetic properties of a representative quantum dot ($Si_{27}M_2H_{36}$) doped with two Mn or Fe atoms (Fig. 1). One TM dopant was placed in the center site, and the other one replaces one silicon atom in another lattice site. The results are listed in Table II. With one TM atom doped in the center site, there are three different doping sites for another TM atom. The distance to the center from near to far are denoted as (a), (b), and (c) in Table II. From the relative energies listed in Table II, it can be seen that the most stable doping site for the second Mn atom is at the outmost of quantum dot and the local moments on Mn-Mn exhibit ferromagnetic (FM) alignment. When the second Mn atom is placed nearby the central Mn atom, the moments of Mn-Mn exhibit antiferromagnetic (AFM) alignment. In the case of Fe doping, the second Fe atom prefers to the core region of the cluster. The two Fe dopants stay close and the alignment of the Fe-Fe spins is ferromagnetic. When the second Fe atom is placed in other sites, the spins of both Fe atoms become zero.

In previous works, the magnetic properties of group-IV semiconductors with dilute magnetic impurities have been investigated.[19–21] Using *ab initio* full-potential augmented plane wave method within the framework of DFT, Stroppa *et al.* studied Mn_xGe_{1-x} and Mn_xSi_{1-x} systems.[19] They considered various concentrations (i.e., x=0.5, 0.25, 0.125, 0.0625, and 0.03125). Irrespective of the content, Mn was found to be a source of holes and the localized magnetic moment is about $3\mu_B$ per atom. Moreover, the FM alignment is favored compared to the AFM one, while the stability generally increases with Mn content. Weng and Dong[20] studied a number of TM-doped group-IV semiconductors, R_xY_{1-x} (R=Cr, Mn, Fe; Y=Si, Ge) by first-principles calculations. For different doping concentrations, each type of TM atoms has almost the identical magnetic moments. The computed magnetic moments are about $2.3\mu_B$/atom for Cr, $2.7-2.8\mu_B$/atom for Mn. For Fe-doped Si at both concentrations of 3.125% and 6.25%, the FM states can exist only in a short R-R range. Except for very short R-R distance, all the configurations for Fe doped in the Si host matrix favor the nonmagnetic independence of the initial magnetic state. While for the Mn-doped Si, the short-range AFM interaction competes with the long-range FM interaction. These results are qualitatively consistent with our present finding. Experimentally, it was found that Mn_xGe_{1-x} (Ref. 22) and Fe_xGe_{1-x} (Ref. 21) are ferromagnetic semiconductors, while the magnetic behavior for Mn and Fe doped in Si still needs further experimental investigations.[20]

C. Interaction between TM dopants and silicon quantum dots

Overall speaking, there is a remarkable reduction of the magnetic moments for the 3*d* and 4*d* transitional-metal atoms when they are doped inside the silicon quantum dots (see Fig. 2). This effect is due to strong hybridization between the 4*s* and 3*d* (5*s* and 4*d*) states of central transitional-metal atom and 3*s* and 3*p* states of Si atoms. The on-site charges of 3*d* (4*d*) atoms from Mulliken analysis are listed in Table I and plotted in Fig. 5. In different quantum dots, similar trends were found. Across the periodic table, the amount of charge transfer from 3*d* (4*d*) atoms to Si host decreases and the direction of charge transfer reverses at Co (Rh). The amount of charges transfer from Si atoms to Co (Rh) atoms is very small (about 0.1), and then the direction of charge transfer becomes from 3*d* (4*d*) atoms to Si atoms and the amount of charge transfer increases again. The behavior of charges transfer in silicon quantum dot is different from that of metal atoms in bare silicon cages without hydrogen passivation, where charges transfer occurs from Si host to the metal atom.[23]

To further discuss the interaction between transition metal dopants and silicon quantum dots, Fig. 4 plots the deformation densities of $Si_{59}H_{60}$, $Si_{58}CrH_{60}$, and $Si_{58}FeH_{60}$ as representatives. The deformation density is calculated from the total electron density subtracted from the corresponding density of the isolated atoms, which can reflect the characteristics of chemical bonding. The blue regions in the deformation density plot indicate the formation of chemical bonds. To discern the difference, the center regions are magnified in the right panel of Fig. 4. It can be seen that in $Si_{59}H_{60}$ the central Si atom forms covalent bonds with the nearest neighboring four Si atoms and the blue region of high deformation density located in the center of Si-Si bonds. When the central Si atom in the $Si_{59}H_{60}$ cluster is substituted by a Cr atom, in addition to the formation of Cr-Si bonds characterized by the blue region in the center, some small fragments of deformation density were observed around the Cr atom. Different

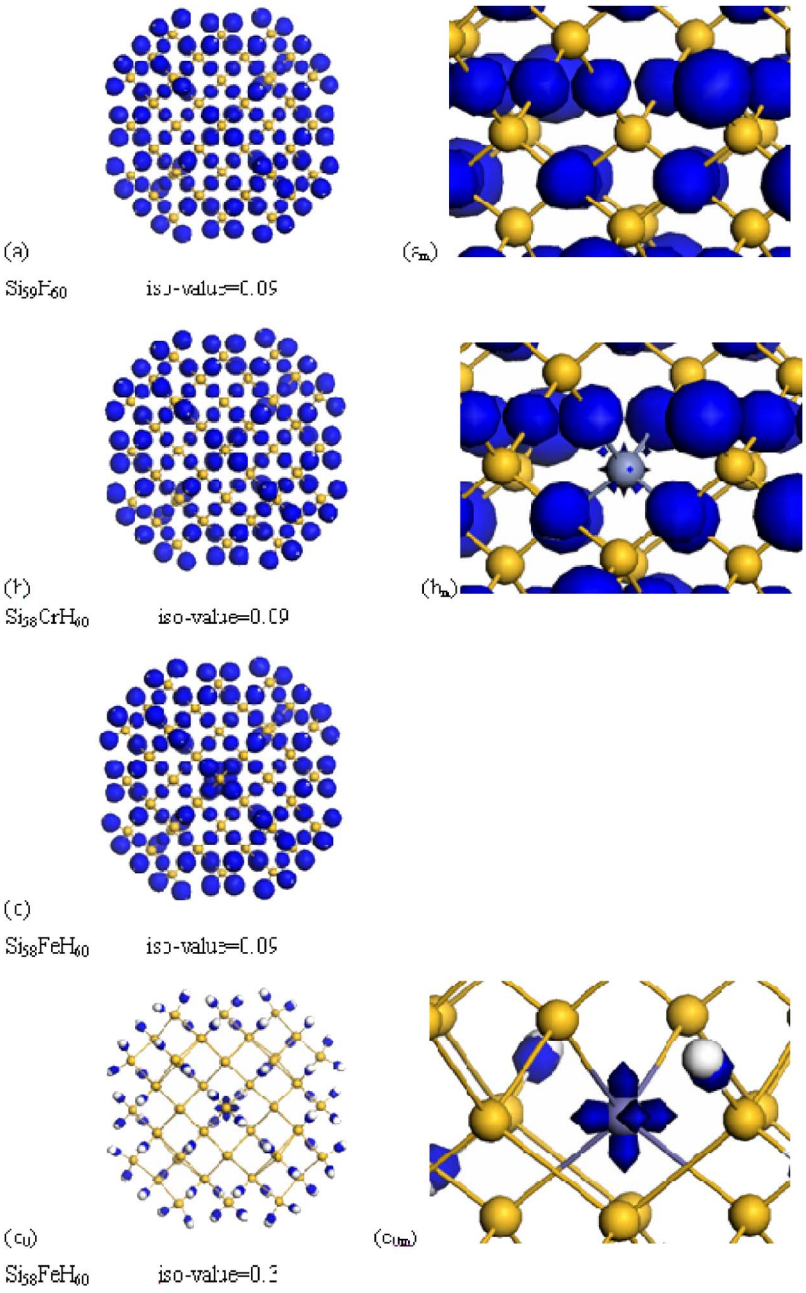

FIG. 4. (Color online) Deformation density of $Si_{59}H_{60}$, $Si_{58}CrH_{60}$, and $Si_{58}FeH_{60}$. The center regions are magnified in plots on the right side. Isovalue: specifies the field value at which the isosurface is drawn.

from that in $Si_{58}CrH_{60}$, the blue region around the Fe atom in $Si_{58}FeH_{60}$ is very clear and large, and some parts of the density distributed around the Fe atom nearly touch, with the density belonging to the Fe-Si bonds. Indeed, the deformation density plotted in the enlarged figure of the central region would be too dense with the isovalue of 0.09. Instead, we plotted the deformation density using the isovalue of 0.3 in Fig. 4 (c_0) and (c_{0m}). With this higher isovalue, the blue regions are reduced greatly. However, around the Fe atom, the distribution of deformation density remains very dense and shows excellent symmetry. To elucidate the reason of the difference in Fig. 4, we analyze the orbital charges transfer in Cr and Fe atoms. The valence electrons in free atom are $3d^5 4s^1$ for Cr and $3d^6 4s^2$ for Fe. After doped in $Si_{59}H_{60}$, the charges of 3*d*, 4*s*, and 4*p* orbits in Cr atom are 4.911, 0.345, and 0.491, respectively; while in Fe atom they are 6.980, 0.546, and 0.361, respectively. There is almost no change of charge distribution for 3*d* orbit of Cr. However, the 3*d* orbit of Fe gains 0.98 electrons, much higher than that of Cr. Such a charge transfer mainly comes from Fe 4*s* state, namely the internal electron transfer occurs for Fe. The different behavior of charges transfer in *d* orbits between Fe and Cr is obviously related to the difference of deformation density in Fig. 4, which also results in the different magnetic behavior of the transitional-metal atoms in silicon quantum dots.

D. Structures and bonding of TM-doped silicon quantum dots

We also discussed the structures and stability of quantum dots with transition-metal doping. From our calculations, the binding energies of all $Si_{n-1}MH_m$ clusters are larger than

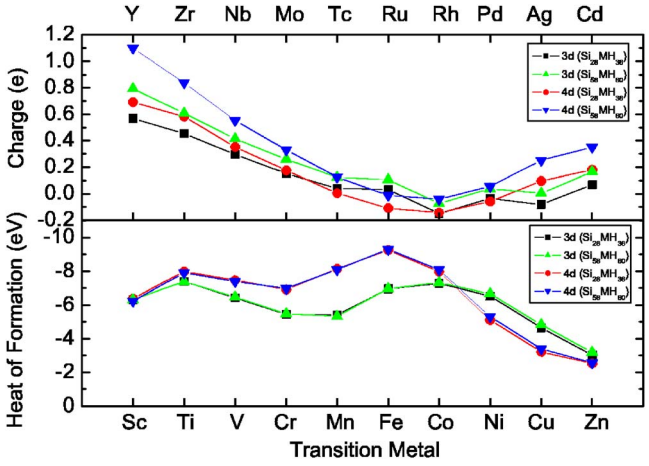

FIG. 5. (Color online) Heat of formation and on-site charges of 3*d* and 4*d* atoms in $Si_{n-1}MH_m$ clusters.

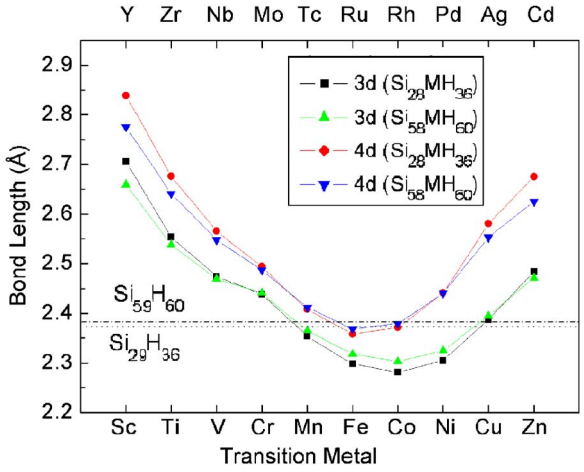

FIG. 6. (Color online) Bond lengths between centered atom and the nearest Si atoms, comparing with the centered Si-Si bond lengths for bare Si_nH_m clusters (dashed lines).

those of $Si_{n-1}H_m$, but less than those of Si_nH_m. This indicates that the doped metal atom can form chemical bond with surrounding Si atoms and stabilize the quantum dots with vacancy. However, due to the mismatch of atomic radius and different nature of Si-Si and Si-*M* bond, doping the Si quantum dots by transition-metal atoms is endothermal.

The heat of formation for a vacancy in the center of silicon quantum dot is also calculated. For the quantum dots of different sizes, the calculated heats of vacancy formation range from 9.1 eV to 9.5 eV. Similar to the definition used in Sec. III B, we also calculated the heat of formation of the 3*d* and 4*d* impurity in the Si quantum dots with a central vacancy. The theoretical results are given in Table I and are plotted in Fig. 5. From Fig. 5, it can be seen that the size of the quantum dots has little effect on the heat of formation. Across the periodic table, the heats of formation of 4*d* impurities are less than those of 3*d* impurities until Co and Rh. The trend is reversed for the later transition elements, that is, the heat of formation of 3*d* atoms is less than that of 4*d* atoms for the last three TM elements.

Combining the heat of formation for the central vacancy in silicon quantum dot with the heat of formation of a TM impurity doped in a silicon quantum dot with a central vacancy, one can derive the substitution energy for forming $Si_{n-1}MH_m$ from Si_nH_m. For all quantum dots and all TM elements studied, we found the substitution energies are always positive. Again, this shows that doping the Si quantum dots by transition metal atoms is endothermal.

Figure 6 plots the bond lengths between the central transition metal atom and the nearest neighboring Si atoms, along with the Si-Si bond lengths in the center of pristine Si quantum dots. From our DFT calculation, the Si-Si bond length in bulk Si is 2.369 Å, while in Si quantum dot it is slightly stretched. For example, the Si-Si bond between the central Si atom and its nearest neighbors are 2.371 Å and 2.382 Å in $Si_{29}H_{36}$ and $Si_{59}H_{60}$, respectively. As shown in Fig. 6, the *M*-Si bond length decreases from ~2.7 Å at Sc to ~2.3 Å at Co for 3*d* transition metals and decreases from ~2.8 Å at Y to ~2.4 Å at Rh for 4*d* transition metals; afterwards, it increases. Except for Mn, Fe, Co, Ni, Ru, and Rh, most *M*-Si bonds are longer than the central Si-Si bonds in the pristine Si quantum dots. The Mn-Si bond lengths (about 2.35 Å) are closest to the bulk Si-Si bond length and the deviation is only about 0.7%. In the Mn-doped Si and Ge ordered alloys, the variations of bond length are at most 1.7%,[20] rather close to present results. The *M*-Si bonds for all the 4*d* elements are longer than those of the 3*d* elements belonging to the same family in the periodic table, due to the larger atomic radius. On the surface of Si quantum dots, the Si-H bonds are nearly 1.5 Å in all the cases, close to the experimental Si-H bond length of 1.48 Å for the SiH_4. Kumar and Kawazoe[24] investigated the H interaction on metal-encapsulated silicon clusters. They found that the adsorption of H weakens the interaction between Si cage and the encapsulated metal atom and leads to distortions in the cages. At present, the geometries of quantum dots remain the T_d symmetry from initial construction after DFT relaxation without symmetry constraint.

IV. CONCLUSIONS

In summary, we have presented first-principles calculations for 3*d* and 4*d* transitional-metal atoms doped in hydrogen-passivated silicon quantum dots. We find the magnetic behavior of the TM impurities is almost independent of the size and shape of the host quantum dots. After being doped inside the $Si_{n-1}H_m$, the magnetic moments of Sc, Ti, Fe, Co, and Ni atoms and their counterpart in 4*d* transition metals, i.e., Y, Zr, Ru, Rh, and Pd, atoms are completely quenched. On the other hand, V, Cr, Mn, Nb, Mo, and Tc impurities inside $Si_{n-1}H_m$ remain magnetic, but the magnitudes of their moments are significantly reduced from those of free atoms. The moments of these 3*d* atoms are higher than those of their 4*d*. The significant reduction or complete quenching of magnetism can be understood by the hybridization between the doped TM atom and its neighboring Si atoms. Doping of TM atoms in different sites of lattice is also considered. It is found that the substitutional center site is most energetically preferred for TM doping. With more than one TM dopant, the most stable doping sites for both

Mn-Mn and Fe-Fe cases exhibit ferromagnetic alignment. When doped with transition-metal atoms, most of the *M*-Si bonds are longer than the Si-Si bond in the pristine quantum dots. Analysis of the heat of formation reveals that substitutional doping the Si quantum dots by transition metal atoms is endothermal. The present calculations provide an interesting way to develop other magnetic species using semiconductor nanostructures.

ACKNOWLEDGMENTS

This work was supported by the National Natural Science Foundation of China (Contracts No. 90206033, No. 10274031, No. 10474030, No. 60478012), and the Foundation for the Author of National Excellent Doctoral Dissertation of China (Contract No. 200421).

*Corresponding author. Email address: zhaojj@dlut.edu.cn

[1] A. Puzder, A. J. Williamson, J. C. Grossman, and G. Galli, Phys. Rev. Lett. **88**, 097401 (2002).
[2] Steven C. Erwin, Lijun Zu, Michael I. Haftel, Alexander L. Efros, Thomas A. Kennedy, and David J. Norris, Nature **436**, 91 (2005), and references therein.
[3] X. Luo, S. B. Zhang, and S. H. Wei, Phys. Rev. B **70**, 033308 (2004).
[4] D. J. Lockwood, A. Wang, and B. Bryskiewics, Solid State Commun. **89**, 587 (1994).
[5] M. V. Wolkin, J. Jorne, P. M. Fauchet, G. Allan, and C. Delerue, Phys. Rev. Lett. **82**, 197 (1999).
[6] T. Takagahara and K. Takeda, Phys. Rev. B **46**, 15578 (1992).
[7] N. A. Hill and K. B. Whaley, Phys. Rev. Lett. **75**, 1130 (1995).
[8] S. Öğüt, J. R. Chelikowsky, and S. G. Louie, Phys. Rev. Lett. **79**, 1770 (1997).
[9] M. Rohlfing and S. G. Louie, Phys. Rev. Lett. **80**, 3320 (1998).
[10] Q. Zhang, J. Costa, and E. Bertran, Phys. Rev. B **53**, 7847 (1996).
[11] I. Vasiliev, S. Öğüt, and J. R. Chelikowsky, Phys. Rev. Lett. **86**, 1813 (2001).
[12] K. Wildberger, V. S. Stepanyuk, P. Lang, R. Zeller, and P. H. Dederichs, Phys. Rev. Lett. **75**, 509 (1995).
[13] S. Y. Yun, G. B. Cha, Y. Kwon, S. Cho, S. C. Hong, J. Magn. Magn. Mater. **272**, 563 (2004).
[14] R. Pandey, B. K. Rao, P. Jena, and J. Newsam, Chem. Phys. Lett. **321**, 142 (2000).
[15] S. N. Khanna, B. K. Rao, and P. Jena, Phys. Rev. Lett. **89**, 016803 (2002).
[16] L. Ma, J. J. Zhao, J. G. Wang, B. L. Wang, Q. L. Lu, and G. H. Wang, Phys. Rev. B **73**, 125439 (2006).
[17] DMol is a density functional theory (DFT) package distributed by Accelrys Inc. [B. Delley, J. Chem. Phys. **92**, 508 (1990)].
[18] J. P. Perdew, K. Burke, and M. Ernzerhof, Phys. Rev. Lett. **77**, 3865 (1996).
[19] A. Stroppa, S. Picozzi, A. Continenza, and A. J. Freeman, Phys. Rev. B **68**, 155203 (2003).
[20] H. M. Weng and J. M. Dong, Phys. Rev. B **71**, 035201 (2005).
[21] S. Choi, S. C. Hong, S. Cho, Y. Kim, J. B. Ketterson, C. U. Jung, K. Rhie, Bong-Jun Kim, and Y. C. Kim, J. Appl. Phys. **93**, 7670 (2003).
[22] Y. D. Park, A. T. Hanbicki, S. C. Erwin, C. S. Hellberg, J. M. Sullivan, J. E. Mattson, T. F. Ambrose, A. Wilson, G. Spanos, and B. T. Jonker, Science **295**, 651 (2002).
[23] P. Guo, Z. Ren, F. Wang, J. Bian, J. Han, and G. H. Wang, J. Chem. Phys. **121**, 12265 (2004).
[24] V. Kumar and Y. Kawazoe, Phys. Rev. Lett. **90**, 055502 (2003).